

## Article

# Bottom-Up Emission Inventory and Its Spatio-Temporal Distribution from Paved Road Dust Based on Field Investigation: A Case Study of Harbin, Northeast China

Lili Li, Kun Wang \*, Zhijian Sun, Weiye Wang, Qingliang Zhao and Hong Qi

Key Laboratory of Urban Water Resource and Environment, Harbin Institute of Technology, School of Environment, Harbin 150090, China; 19B329017@stu.hit.edu.cn (L.L.); 20S129110@stu.hit.edu.cn (Z.S.); 16B927084@stu.hit.edu.cn (W.W.); qlzhao@hit.edu.cn (Q.Z.); hongqi@hit.edu.cn (H.Q.)

\* Correspondence: wangkun02@hit.edu.cn

**Abstract:** Road dust is one of the primary sources of particulate matter which has implications for air quality, climate and health. With the aim of characterizing the emissions, in this study, a bottom-up approach of county level emission inventory from paved road dust based on field investigation was developed. An inventory of high-resolution paved road dust (PRD) emissions by monthly and spatial allocation at 1 km × 1 km resolution in Harbin in 2016 was compiled using accessible county level, seasonal data and local parameters based on field investigation to increase temporal-spatial resolution. The results demonstrated the total PRD emissions of TSP, PM<sub>10</sub>, and PM<sub>2.5</sub> in Harbin were 270,207 t, 54,597 t, 14,059 t, respectively. The temporal variation trends of pollutant emissions from PRD was consistent with the characteristics of precipitation, with lower emissions in winter and summer, and higher emissions in spring and autumn. The spatial allocation of emissions has a strong association with Harbin's road network, mainly concentrating in the central urban area compared to the surrounding counties. Through scenario analysis, positive control measures were essential and effective for PRD pollution. The inventory developed in this study reflected the level of fugitive dust on paved road in Harbin, and it could reduce particulate matter pollution with the development of mitigation strategies and could comply with air quality modelling requirements, especially in the frigid region of northeastern China.

**Keywords:** paved road dust; bottom-up; emission factors; emission inventory; spatio-temporal distribution; Harbin



**Citation:** Li, L.; Wang, K.; Sun, Z.; Wang, W.; Zhao, Q.; Qi, H. Bottom-Up Emission Inventory and Its Spatio-Temporal Distribution from Paved Road Dust Based on Field Investigation: A Case Study of Harbin, Northeast China. *Atmosphere* **2021**, *12*, 449. <https://doi.org/10.3390/atmos12040449>

Academic Editor: Begoña Artíñano

Received: 11 March 2021

Accepted: 30 March 2021

Published: 31 March 2021

**Publisher's Note:** MDPI stays neutral with regard to jurisdictional claims in published maps and institutional affiliations.



**Copyright:** © 2021 by the authors. Licensee MDPI, Basel, Switzerland. This article is an open access article distributed under the terms and conditions of the Creative Commons Attribution (CC BY) license (<https://creativecommons.org/licenses/by/4.0/>).

## 1. Introduction

Pollution by particulate matter (PM), which has adverse effects on human health, is considered to be a pivotal reason of poor urban air quality in China [1,2]. Since 2010, Northeast China has gradually developed into the fifth largest smog area in China. Harbin has been experiencing serious air pollution the heating period of recent years, raising more concerns about air quality improvement. Emission inventory with highly resolved spatio-temporal profiles are desperately needed, which are essential for the sources of air pollution emissions and facilitating the development of significant air pollution control strategies [3,4]. Researchers and policymakers have been focusing on emission inventory for the past few decades. Air pollutant emission inventory at different pollution sources have been established in China, covering roads and motor vehicles [5], biomass burning [6,7] and so on. So far, however, few studies have reported fugitive dust emission inventory. China has made efforts in developing source emission inventory. Nine technical guides, such as “The Technical Guide of Compiling Particulate Matter Emission Inventory from Fugitive Dust Source (Trial Version)” (hereinafter referred to as the Guide) were issued by the Ministry of Environment Protection of China in 2014 (<http://www.mee.gov.cn/gkml/hbb/bgg/201501/W020150107594588131490.pdf>).

Fugitive dust from soil, paved and unpaved roads, buildings and cement has been identified as a significant source of urban PM pollution, second only to fuel combustion and the formation of secondary organic aerosols [8,9], particularly in dry and semiautid areas [10]. In 14 Chinese cities, fugitive dust accounted for 12~34% of winter PM<sub>2.5</sub> mass and 17~32% of summer PM<sub>2.5</sub> mass [11]. The emissions of fugitive dust are episodic and widely fluctuating.

Road dust, which is generated by turbulence or wind, is the predominant form of fugitive dust in urban areas [12,13]. According to the empirical approach proposed in the AP-42 documents of the United States Environmental Protection Agency [14,15], we assessed an average PM<sub>10</sub> emission of 30 g km<sup>-1</sup> for a car with an average weight of 2 tons and an average silt loading of 100 gm<sup>-2</sup> on paved roads, assuming an average load of 30 g km<sup>-1</sup>. Thus, each vehicle traveling 40 km per day, 5 days per week, would release 312 kg of PM<sub>10</sub> per year. As a result of the fast process of urbanization in China, the overall length of the road network is expanding at an increasingly rapid pace, resulting in an ever-increasing amount of dust emissions in the city [16].

In Northern China, dry climate is favorable for fugitive dust emissions, especially in fall and winter [17]. The uneven regional development in China also has also resulted in developing different environmental measures, which leads to making difference in fugitive dust emissions subsequently [18–20]. Harbin, known as “ice city”, is the highest latitude provincial capital city in China and has the continental monsoon climate in the middle temperate zone. July to August is defined as damp, rainy summer and October to March as winter that is cold and dry. Its mean annual temperature was 3.5 °C. By the end of 2016, Harbin had 1,458,000 motor vehicles, which had more fugitive dust seriously in both sides of the road. Meantime, area of paved roads increased from 23.89 million in 2005 to 54.22 million in 2016 (<http://www.stats-hlheb.gov.cn/>). Harbin is representative of the cold northern regions of the city with dust emission. Because of the unique geographic characteristics, there are limited information on a high spatial-temporal resolution PRD source emissions in region scales. Hence, the study on PRD emission inventory can provide critical input for air quality model, and ultimately, it is crucial for the government to formulate reasonable and practical dust control policies to minimize PM levels and promote air quality in Harbin. Meantime, it can provide a reference for developing road dust emission inventory in cold northern regions.

Both bottom-up and top-down methods can be used to develop emission inventory. However, emissions at the county resolution are considerably better to represent the actual situation [21]. For provincial level emission inventory, the whole city’s total emission was often allocated according to population or other factors, which would bring uncertainty. Emission inventory of air pollutants at county level are necessary, however, there have been fewer reports of the PRD emission inventory based on districts and country emitters. So, the bottom-up method is more appropriate and widely used at provincial or county level.

In the present study, we aimed at developing a 1 km resolution inventory on air pollutants from paved road dust based on field investigation in Harbin using the bottom-up approach. The methodology and process of developing dust inventory can be used as a guide for other cities to carry out inventory development. Here, to supplement key missing parameters in estimating domestic PRD emissions, several parameters influencing emissions factors were determined based on field investigation. Then we sought to develop a district-based emission inventory of the PRD with high spatial resolution, analyzed the spatio-temporal characteristics of Harbin’s PRD emissions and developed scenario analysis of PRD control policy. The complete and systematic research for the high spatial resolution PRD emission inventory was acquired.

## 2. Methodology

### 2.1. Description of Harbin City

Harbin (125.4~130.1° E, 44.0~46.4° N), capital of Heilongjiang province, is located at the northernmost of Northeast China Plain, with a total area of 53,100 km<sup>2</sup> and a population

of about 10.7 million. Harbin administers 9 municipal districts (Daoli, Nangang, Daowai, Pingfang, Songbei, Xiangfang, Hulan, Acheng, Shuangcheng), 7 counties (Yilan, Fangzheng, Bin, Bayan, Mulan, Tonghe, Yanshou), and 2 county-level cities (Shangzhi and Wuchang), which has set up 13 meteorological stations (Figure 1a). This study uses Daoli, Daowai, Nangang, Xiangfang, Pingfang, and Songbei as a central urban area according to the setting of the meteorological stations. Background information about meteorology obtained from Harbin Meteorological Administration was shown in Appendix A (Tables A1 and A2). The network of paved road in Harbin was shown in Figure 1b.

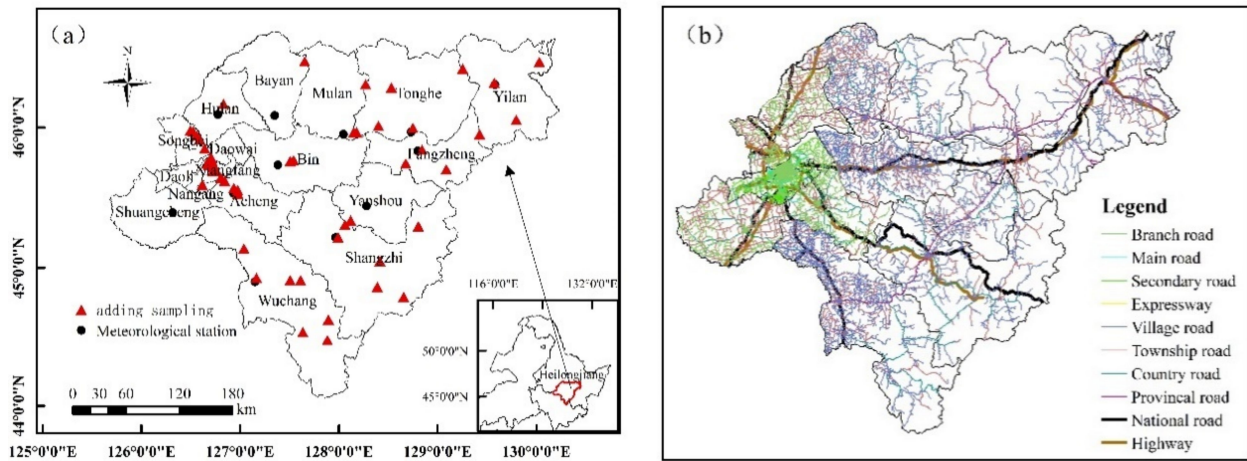


**Figure 1.** The geo-location of the studying area. (a) Regional division, meteorological stations and sampling locations in Harbin, (b) The network of paved road in Harbin.

### 2.2. Computational Methods

PRD emission inventory can be established in this study using a bottom-up approach (Figure 2). The method that calculated paved road dust (PRD) emission inventory is listed in the Guide, which is based on emission factors. According to the Guide, paved roads were defined by two primary types or 10 secondary types (Table 1). We first calculated the combined air pollutant emission factors for individual paved road types. Then, we integrated with the 2016 traffic-flow and road-length data for every district, the PRD emissions were estimated by the district. The PRD emissions of TSP, PM<sub>10</sub> and PM<sub>2.5</sub>, for each type of paved section in each region, were calculated using the following equations based on AP-42 with updated parameters [13,22]:

$$W_{Pi} = E_{Pi} \times L_{Pi} \times N_{PR} \times \left(1 - \frac{n_{Pr}}{365}\right) \times 10^{-6} \tag{1}$$

$$E_{Pi} = k_i \times (sL)^{0.91} \times W^{1.02} \times (1 - \eta) \tag{2}$$

where the emissions of PRD ( $W_{Pi}$ , t/a) relies mainly on the emission factor ( $E_{Pi}$ , g/(km·veh), the length of road  $i$ , in region  $R$  ( $L_{Pi}$ , km), the average vehicle flow on this section of the road for a certain period ( $N_{PR}$ , veh/a) and the number of days without dust ( $n_{pr}$ ).  $E_{Pi}$  is the emission rate of size-specific PM (same units as  $k_i$  (g/km));  $sL$  is the silt load (g/m<sup>2</sup>);  $W$  is the average weight of the fleet (tons), which can be established based on the ratio and the weight of different type of vehicles;  $\eta$  is the control efficiency (%).

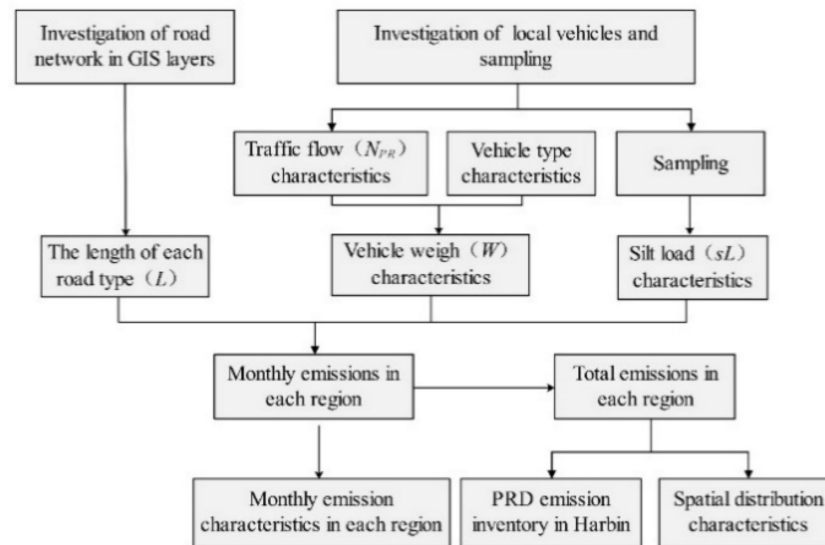


Figure 2. Technical route of developing PRD emission inventory.

Table 1. The types and length of paved roads in Harbin.

Primary Types	No.	Secondary Types	Road Length (km)
Public road	1	Highway	902
	2	National Road (NR)	996
	3	Provincial Road (PH)	731
	4	County Road (CR)	1915
	5	Township Road (TR)	9009
	6	Village Road (VR)	9332
Urban road	1	Expressway	60
	2	Main Road (MR)	647
	3	Secondary Road (SR)	1840
	4	Branch Road (BR)	3972

In Equation (1),  $L_{pi}$  was based on GIS maps of the road network.  $N_{PR}$ ,  $W$  and  $sL$  were obtained through field investigation.  $n_{pr}$  was counted by meteorological data in Harbin in 18 districts.  $k_i$  is the scale factor for PM mass (i.e., TSP,  $PM_{10}$ ,  $PM_{2.5}$ ), adopting 3.23, 0.62 and 0.15 in this study referenced to the Guide.  $\eta$  is another crucial influence associated with dust emissions, primarily considering the abatement effect of control measures. Combined with road type and practical dust control measures in Harbin, dust control measures on urban roads (i.e., Expressway, Main Road, Secondary Road, Branch Road) included regular snow and sprinkler cleaning. The dust control measures on public roads (i.e., Highway, National Road, Provincial Road, County Road, Township Road, Village Road) were just snow cleaning in winter and no dust control measures in other seasons.

### 2.3. Investigation of Activity Level

According to Equation (1), activity level is developed to obtain  $L_{pi}$ ,  $N_{PR}$  and  $n_{pr}$ . Adding the processed road network to the ArcGIS layer according to the road types in Table 1,  $L_{i,R}$  was obtained in Table A3. Combined with the daily precipitation in 2016 at 13 meteorological stations in Harbin,  $n_{pr}$  can be expressed as the number of days in the year with rainfall greater than 0.25 mm/d, as was in Table A4.

In addition to the above two parameters, traffic flow was an essential indicator for the level of motor vehicle activity [23]. To estimate emissions of fugitive dust from paved road vehicles, the investigation was performed from 12 July to 13 July in 2016, to guarantee the traffic flow data are as representative as possible. Traffic observations were recorded three times a day for 20 min in the morning, noon and evening, respectively. Then we

expanded the recording data, depending on the traffic daily flow curve from Harbin Traffic Management Department. Meantime, we also counted vehicle types on different types of road in the process of investigation.

#### 2.4. Localization of Silt Load

The consideration of the effect of velocity on emissions is reflected by the parameter silt loading. Silt loading values are highly related to anthropogenic activities [24,25]. Based on Equation (2), this paper through sampling and research localizes emission factors for PRD. PRD emissions had been found to vary according to the silt load [26]. Therefore, we determined silt load in Harbin by sampling. The sampling site map was shown in Figure 1a, representing the road section covering 10 road types. Sampling points were distributed in each district in Harbin, and a total of 56 road dust samples were obtained from October to December 2016. The following formula was applied to calculate the localized  $sL$ .

$$sL = \frac{W_T - W_{20} - W_{200}}{W_T} \times \frac{W_0}{S} \quad (3)$$

where  $W_0$  (g) is the mass of PRD after dried, The dust  $W_T$  (g) of about 30~100 g were passed through 20 and 200 mesh sieves (corresponding hole diameter 0.850 mm and 0.075 mm) in sequence. The dust samples on the 20 and 200 mesh sieve were denoted as  $W_{20}$  (g) and  $W_{200}$  (g), respectively.

#### 2.5. Spatial and Temporal Allocation

The distribution of total emissions to gridded cells is a key protocol for the development of high-resolution emission inventory. Logical and appropriate spatial allocation methods will facilitate the reduction of uncertainties in the establishment of temporal and gridded emissions, resulting in improved model properties [27–29]. To improve the spatial resolution, 1 km × 1 km grids were implemented. Total emission inventory was allocated by GIS to the corresponding grid according to the road network (Figure 3). Finally, the PRD emissions for each region are calculated by adding up the emissions from all 1 km grid cells within the corresponding region.

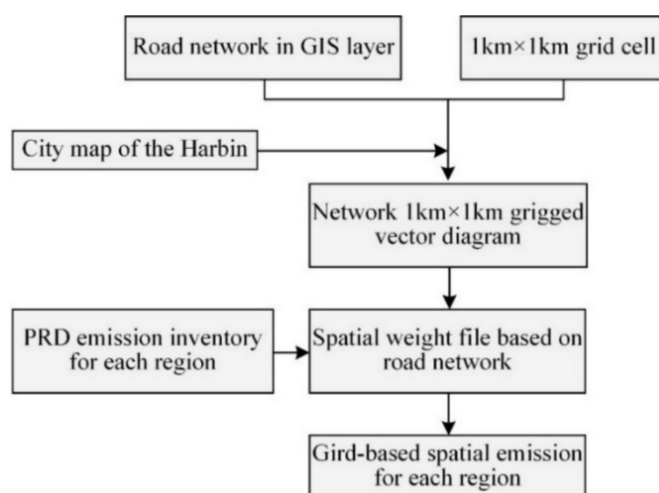


Figure 3. Flowchart of spatial allocation for PRD emissions.

Meteorology can have a significant influence on concentrations by means of surface and diffusion conditions [30]. Hence, we chose the number of days without dust as temporal allocation factor based on Equation (2) afterwards, the monthly PRD emissions be calculated based on Table A4.

### 3. Results and Discussion

#### 3.1. Emission Inventory of PRD in Harbin in 2016

##### 3.1.1. Vehicle Flow and Type

Average daily traffic volumes and vehicle types vary by road type, as shown in Figure 4. The average traffic flow in Harbin was Expressway > MR > SR > NR > CR > PR > Highway > TR > BR > VR, daily traffic flow on urban roads was noticeably more massive than that on public road, mainly owing to the larger number of motor vehicles in urban areas. Vehicle types for different road types differ significantly, but for all road types, minibuses accounted for the largest proportion, which accounted for 45.68% to 72.28% of total traffic on highways, and 59.83~66.19% of total traffic on urban roads.

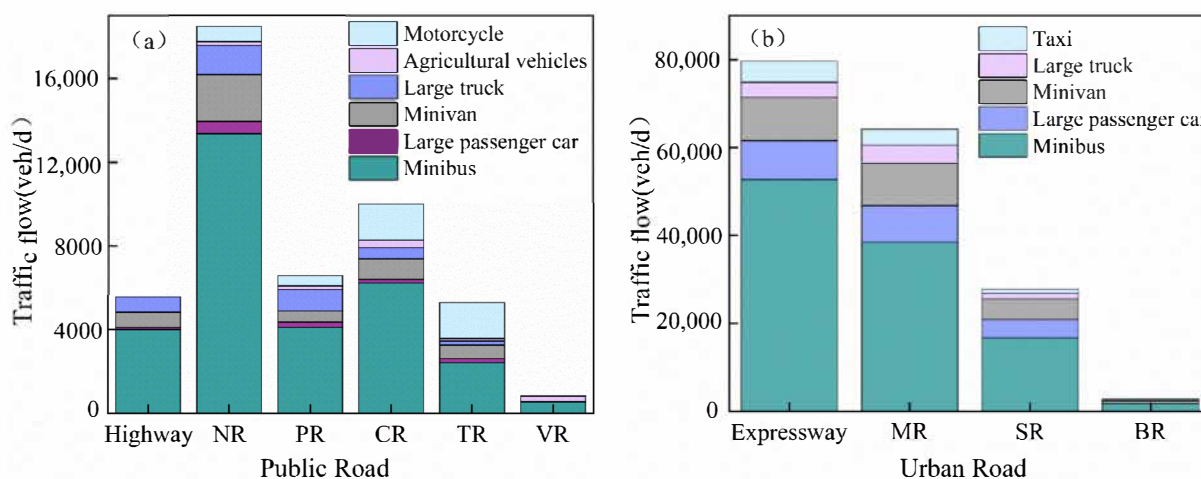


**Figure 4.** Traffic flow and vehicle types for all secondary types of paved roads. (a) Traffic flow on public roads, (b) Traffic flow on urban roads.

##### 3.1.2. Silt Load and Vehicle Weight

Firstly, based on the above information of traffic flow and vehicle type, the average vehicle weight of various road types in Harbin was calculated (Table 2). The average vehicle weight order of each grade paved road in Harbin was SR > MR > PR > Expressway > Highway > NR > BR > CR > TR > VR. The average vehicle weight of urban roads was higher than that of highways, which is mainly due to the massive traffic volume of urban roads and the relatively large number of large cargo and passenger vehicles.

**Table 2.** Average vehicle weight ( $W$ , t) and silt load ( $sL$ ,  $g/m^2$ ) in Harbin.

Types	Highway	NR	PR	CR	TR	VR	Expressway	MR	SR	BR
$W$	3.34	2.91	3.51	2.38	2.17	1.98	3.42	3.76	3.78	2.57
$sL$	0.94	0.92	1.18	1.02	1.26	1.14	0.32	0.38	0.53	1.38

After laboratory analysis and treatment of the samples,  $sL$  of each paved road type in Harbin were obtained according to Equation (3) (Table 2).  $sL$  in Harbin was BR > TR > PR > VR > Highway > CR > NR > SR > MR > Expressway, which is similar to that of the Pearl River Delta [31]. Meantime, the relationship between silt load and traffic flow was obtained (Figure 5). Except for highway and VR, there was a negative correlation between traffic flow and silt load for other road types. The larger the traffic flow, the smaller the silt load. The main concern is that silt load is concerned with particles with smaller particle sizes easily carried into the air by the airflow generated by the motor vehicle during driving. And the traffic flow of urban roads is much larger than that of public roads besides high frequency of road cleaning in urban areas. Therefore, the road traffic volume was large, while the road surface was less dusty, resulting in lower silt load.

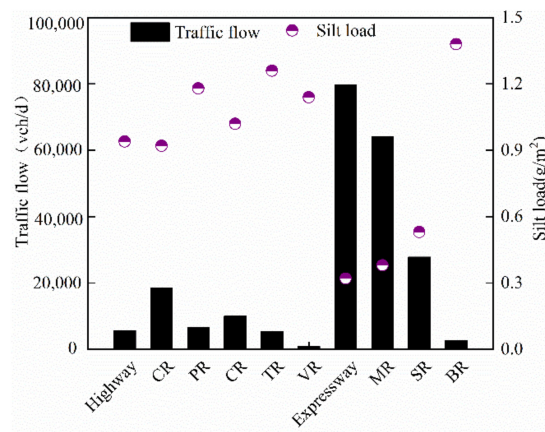


Figure 5. The relationship between silt load and traffic flow in Harbin.

### 3.1.3. Emissions Factor

Based on Sections 3.1.1 and 3.1.2 measured data of *sL* and *W*, the emission factors of PM were obtained for each road type in 18 districts according to Equation (2). The annual dust emission factors for each road type were selected, as shown in Figure 6.

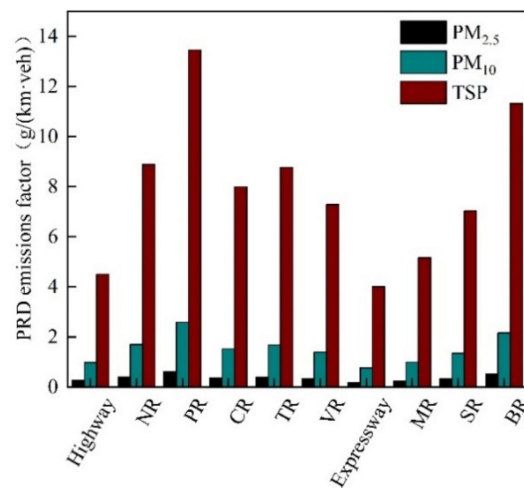


Figure 6. PRD emissions factor in Harbin.

From above, it can clearly be noted that the emission factors of PM<sub>2.5</sub>, PM<sub>10</sub> and TSP on expressway were the smallest, with 0.186, 0.771, and 4.014 g/(km·veh), respectively, and the highest emission factors for PRD on paved road., which were 0.625, 2.584, 13.463 g/(km·veh) respectively. In terms of urban roads, PM<sub>10</sub> and PM<sub>2.5</sub> of the BR had the largest emission factors, which were 0.526 and 2.173 g/(km·veh), respectively. This conclusion was close to that of Chengdu’s road dust emission factors, whose emission factors of PM<sub>10</sub> and PM<sub>2.5</sub> of the BR were 0.28 and 1.15 g/(km·veh), respectively [32].

### 3.1.4. Emission Inventory by Road Type of PRD

In 2016, the total PRD emissions of TSP, PM<sub>10</sub>, and PM<sub>2.5</sub> were 270,207 t, 54,597 t, 14,059 t in Harbin, respectively. Table 3 showed the contributions of each road type to the total PRD emissions in Harbin.

**Table 3.** PRD emission inventory in different road types in Harbin in 2016 (t).

Road Types	PM <sub>2.5</sub>	PM <sub>10</sub>	TSP
Highway	434	1677	8035
NR	1567	6201	30758
PR	601	2374	11759
CR	1441	5710	29748
TR	4081	16214	84472
VR	553	2197	11409
Expressway	135	498	2262
MR	1446	5292	23763
SR	2495	9203	41743
BR	1306	5229	26258
Total	14059	54597	270207

PM<sub>2.5</sub>, PM<sub>10</sub> and TSP emissions proportion of TR were the largest, with 29.03%, 29.70% and 31.26%, respectively. It was mainly higher activity level in TR, whose length ranks second in the total length of all road types in Harbin. Expressway was the smallest, accounting for 0.96%, 0.91% and 0.84% of PM<sub>2.5</sub>, PM<sub>10</sub> and TSP total emissions, due to their emission factors and activity level at the bottom of each road type. In China, all highways and urban roads were protected against dust accumulation with trees, buildings, barriers etc. In addition, studies had shown that exhaust emissions were concentrated in urban centers and on highways. And the dust studied in this paper showed such characteristics. Exhaust and non-exhaust emissions were still mainly distributed in densely populated areas [33]. Although the total length of the VRs was the largest, there were mostly paved with cement. The silt dust and traffic flow of VRs were lower so that the emission factor was lower, eventually leading to smaller dust emission.

### 3.1.5. Discussion of the Reliability in the Emission Estimation

The uncertainty of the PRD emission inventory arises mainly from activity levels and emission factors, given the lack of lack of understanding of activity data and emission factors, or inaccurate or imprecise estimates of these data [33,34]. we conducted a qualitative analysis of uncertainty through comparisons with other cities to determine sources of uncertainty in the inventory, then the results were shown in Table 4.

**Table 4.** Comparison with other studies (t).

City	Object	Year	PM <sub>2.5</sub>	PM <sub>10</sub>	TSP	Reference
Huhhot	All roads	2006	5400	22,000	115,000	[35]
Tianjin	Urban roads	2010	1300	5372	27,985	[36]
Nanjing	Urban roads	2014	16,030	67,270	-	[37]
Chengdu	All roads	2012	11,793.26	48,745.26	-	[32]
Beijing	All roads	2012	13,565	-	-	[38]
Pearl River Delta	Public roads	2011	127,900	528,800	2,755,100	[31]
This study	All roads	2016	14,059	54,597	270,207	-

The activity level each road type relies on the road network and area statistics of the traffic flow and meteorological data. The emission factors of each road type were computed from multiple parameters involving  $sL$  and  $W$ . The coefficients of PM and control efficiency were all selected as a consistent value for different districts.

Also, while many efforts have been taken to update emission inventory, uncertainty is inevitable. Emissions also differ from place to place because of differences in climate, road characteristics and traffic conditions. The suggestions reducing PRD emission inventory should be further strengthened: Firstly, bottom-up studies can be conducted about the  $N_{PR}$ ,  $sL$  and  $W$  by expanding the survey samples and covering different seasons or even in different months, to evaluate the uncertainty range of each parameter for quantitative

analysis. Secondly, the treatment of the road network needs to be further refined. There were differences between road planning and actual road functions. Hence, confirming that the classification of various types of roads makes it tally with Harbin’s real situation.

### 3.2. Temporal Distribution Characteristics of PRD Emission

Next, we assigned monthly changes in specific domestic PRD emissions for each region. Figure 7 showed the difference in monthly emissions for the PRD region in 2016. We found that the monthly emission trends were similar across the regions over the study period. PM<sub>2.5</sub> and PM<sub>10</sub> emissions from paved roads had a small fluctuation in the whole year compared to TSP. Still, the overall change trends of the three types of particles were relatively consistent, with lower emissions in winter and summer, and higher emissions in spring and autumn. During the summer, as precipitation and vegetation coverage increased, PRD was significantly suppressed. In spring, as snow and ice melted, road dried up and wind speed increased, leaving large amounts of dust for suspension [12].

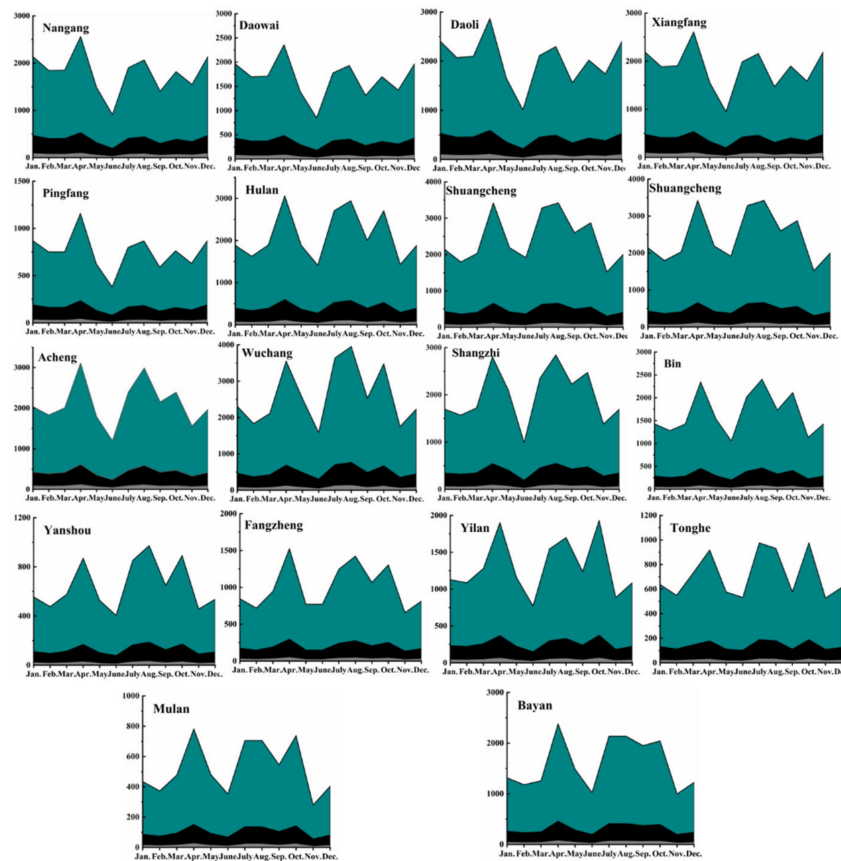


Figure 7. Monthly variations of PRD in Harbin, 2016.

During the study period, in all regions there is an initial tendency to increase, then decreasing, following by a increase, subsequently declined and again during the research period. For most of the districts, three prominent emission peaks for emitted dust from paved road were presented for months in April, August and October, respectively. Mean-time, three nadirs in June, September and November, respectively. In April, wind speeds were higher, and vegetation coverage was lower so that soil dust from both sides of the road was carried to the road. In June, precipitation was the highest in the year and brought the lowest PRD emissions. The reasons for the high dust in autumn were related to the increase in autumn harvest and traffic flow. Moreover, ice, snow and damp road texture were responsible for low road dust emissions from December to February during cold, wet winter weather conditions, which greatly reduced dust emissions.

According to Figure 7, we constructed PRD emission inventory in Harbin based on the districts, as shown in Table 5. The emission intensity of the PRD is higher in urban areas, especially the Xiangfang. Further, the higher emission intensity in urban was the result of the following causes: (1) the high level of urbanization in the central urban area, the road paving area was much larger than that in the suburbs. (2) The economic level and population density in urban areas were higher, resulting in a greater travel demand; Xiangfang District is the center of Harbin's politics, economy, culture, transportation, and information, and the population density is higher, leading to a greater demand for bus transportation than other districts. (3) During the winter snow season in Harbin, the snow clearing mechanism of suburban highways was far inferior to that of urban areas, and road dust was greatly suppressed.

**Table 5.** PRD emission from Harbin districts in 2016.

Districts	PM <sub>2.5</sub>	PM <sub>10</sub>	TSP
Nangang	989	3690	17,010
Daowai	913	3412	15,766
Daoli	1111	4132	19,007
Xiangfang	1017	3800	17,568
Pingfang	410	1534	7120
Hulan	1025	4041	20,380
Shuangcheng	1151	4573	23,488
Songbei	668	2620	13,132
Acheng	1040	4071	20,331
Wuchang	1243	4932	25,335
Shangzhi	950	3759	19,166
Bin	788	3119	16,011
Yanshou	305	1211	6257
Fangzheng	485	1918	9695
Yilan	629	2485	12,605
Tonghe	341	1349	6861
Mulan	247	980	5055
Bayan	747	2969	15,420
Total	14,059	54,597	270,207

### 3.3. Spatial Distribution Characteristics of PRD Emission

After the emission inventory analysis at districts level, we've made spatial distribution according to Section 2.5 to determine the spatial distribution of PRD emissions from Harbin. Generally, spatial allocation of PRD emissions in Harbin was scattered (Figure 8). From the emission area, the network distribution of PRD was the same as that of Harbin's road network. There was a strong correlation between the spatial distribution of emissions and the location of Harbin's road network. That is, the spatial distribution characteristics were similar to the study in Beijing [39,40], with emissions centralized in city centers, mainly due to differences in the structure of the road network. Harbin had formed a circular and criss-crossing road network that creates a high concentration of traffic flows in the center, which is prone to traffic congestion and also results in a gradual decrease in the intensity of vehicle emissions from the city center outward [41]. The PRD emission areas in nine counties were relatively sparse compared to the nine districts, mainly in the south of Wuchang, the eastern part of Shangzhi, and the west of Tonghe and Mulan. Due to the low coverage of paved roads, there were less dust emissions from paved roads. However, it is worth mentioning that this study did not take into account the unpaved road dust, to assess the impact of road dust comprehensively, it is necessary to evaluate the unpaved road dust further.

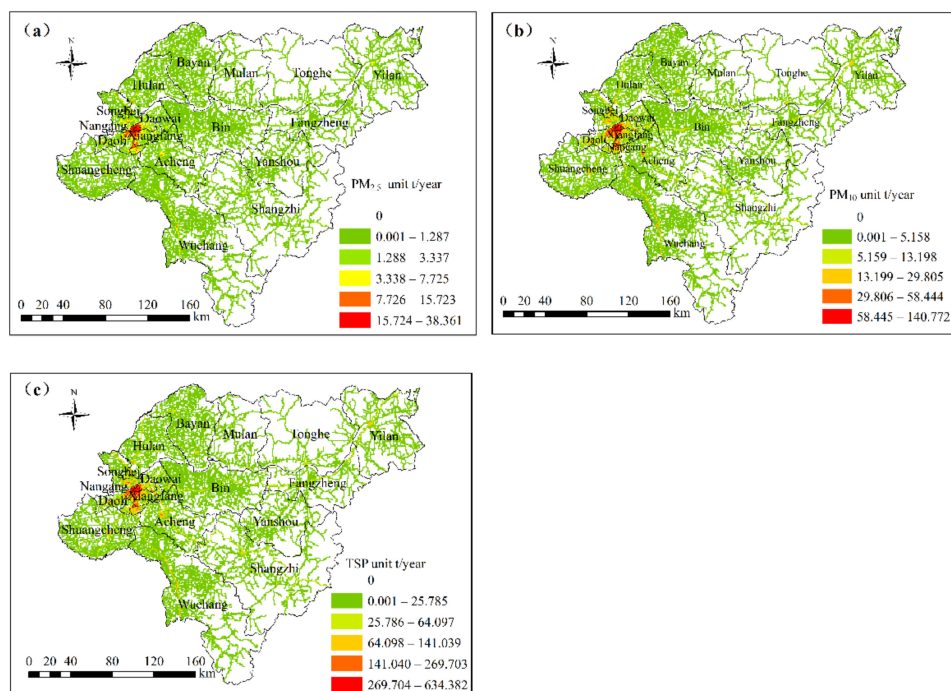


Figure 8. Spatial allocation of PRD in Harbin, 2016. (a) PM<sub>2.5</sub>; (b) PM<sub>10</sub>; (c) TSP.

In this study, the hierarchical road network was used only as spatial representation data for spatial distribution, which will lead to an underestimation of the distribution results in traffic-intensive areas. In fact, many factors, such as traffic flow and the composition of vehicles, will affect the spatial distribution of PRD. The method of spacing allocation of “standard road length” was proposed in the Pearl River Delta [42]; therefore, the space allocation of PRD can be combined with multiple factors in the further study.

### 3.4. Scenario Analysis of PRD Control Policy

The Guide pointed out four kinds of PRD control measures and control efficiency, including road sprinkling, spraying dust suppressant, non-vacuum cleaning and vacuum cleaning. Among them, road sprinkling and spraying dust suppressant had wide applicability. In this study, the baseline scenario was assumed to be non-management strategy except for natural dust suppression measures. Scenario settings were as follows (Table 6) according to “The Guide”: (1) Scenario 1: sprinkle water twice a day; (2) Scenario 2: spraying dust suppressant; (3) Scenario 3: place hedges/trees/barriers alongside the road.

Table 6. Scenario setting for PRD emission amounts in Harbin in 2016.

Scenario Setting	$\eta_{PM_{2.5}}$	$\eta_{PM_{10}}$	$\eta_{TSP}$
Scenario 1	46	55	66
Scenario 2	30	40	48
Scenario 3	52	63	75

PRD emissions under the set-up scenario were calculated (Figure 9). PRD emissions of PM<sub>2.5</sub>, PM<sub>10</sub>, and TSP under the baseline scenario were 20,277 t, 83,812 t and 436,636 t, respectively. The effect of hedges/trees/barriers alongside the road in the measures taken was better than that of sprinkling twice a day and spraying dust suppressants. If all paving roads were guaranteed to be sprinkled twice a day, the emissions of PM<sub>2.5</sub>, PM<sub>10</sub> and TSP in the baseline scenario were reduced by 42.42%, 48.66% and 54.66%, respectively. It can be seen that PRD was controllable, so positive control measures were essential and effective for PRD pollution.

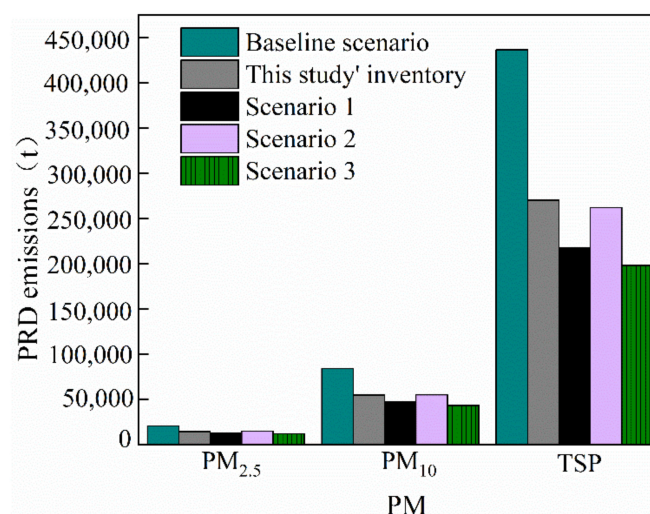


**Figure 9.** PRD emission scenario analysis.

In the practical application, PRD pollution control should take full account of many factors, such as control cost, regional difference and maneuverability. Measures such as Road greening, road hardening, reduction of road damage, removal of road construction, closed transportation and so on can be selected comprehensively according to the local situation so that the emission reduction of dust can be carried out in a targeted and comprehensive way.

#### 4. Conclusions

There are few detailed studies on the estimation of domestic PRD emissions and its spatio-temporal variations due to inadequate information on several critical parameters relevant to PRD estimation up to now. This severely restricts the application air quality models and effective control strategies of fugitive dust for the government. Here, this study attempted to establish a 2016 high-resolution emission inventory for PRD using a bottom-up approach of county level based on field investigation. A 1 km resolution inventory for Harbin, Northern China, was established as a case study, the total PRD emissions of TSP, PM<sub>10</sub>, and PM<sub>2.5</sub> in Harbin in 2016 were 270,207 t, 54,597 t, 14,059 t, respectively. Though many attempts had been made to update the emission inventory, including up-to-date EF and detailed activities data, uncertainty could not be eliminated, the comparison to previous studies demonstrated that this study's emission was relatively credible. The monthly trends for most of the districts, three obvious emission peaks for emitted dust from paved road were presented for months in April, August and October, respectively. Meantime, three nadirs in June, September and November, respectively. The spatial variation at high-spatial resolution (1 km × 1 km) illustrated that the PRD emission areas mainly concentrated in the central urban area compared to the surrounding counties. The south of Wuchang, the eastern part of Shangzhi, and the west of Tonghe and Mulan were always characterized by low emissions. Through scenario analysis, positive control measures were essential and effective for PRD pollution. Consequently, the inventory can comply with air quality modeling requirements and develop effective fugitive dust control strategies for governments, particularly in dust-dominated regions like Harbin and other cold areas in China.

**Author Contributions:** Conceptualization, L.L., K.W. and Q.Z.; methodology, L.L.; writing—original draft preparation, L.L. and Z.S.; writing—review and editing, Z.S. and W.W.; supervision, Q.Z. and H.Q.; Funding acquisition, K.W. and H.Q.; All authors have read and agreed to the published version of the manuscript.

**Funding:** This work was supported by the Open Project of State Key Laboratory of Urban Water Resource and Environment, the Harbin Institute of Technology (No. 2016TS08); Heilongjiang Provincial Government Procurement Center: emission inventory of high-resolution dust sources in Harbin (No. SC [2017] 2134).

**Institutional Review Board Statement:** Not Applicable.

**Informed Consent Statement:** Not Applicable.

**Data Availability Statement:** Not Applicable.

**Conflicts of Interest:** The authors declare no conflict of interest.

## Appendix A

Table A1. Average monthly wind speed in 2016 at 13 meteorological stations (m/s).

Month	Acheng	Bayan	Bin	Fangzheng	Urban	Hulan	Mulan	Shangzhi	Shuangcheng	Tonghe	Wuchang	Yanshou	Yilan
January	1.731	3.015	2.609	3.508	2.331	2.467	2.639	3.016	3.482	3.994	2.649	3.268	5.719
February	2.162	3.532	2.483	3.088	2.521	3.018	2.994	2.706	4.314	3.670	3.221	3.135	3.896
March	2.695	4.846	3.593	3.502	3.366	4.114	4.039	3.331	5.397	4.440	4.068	4.040	4.253
April	3.312	5.792	4.239	4.248	3.946	4.915	4.964	4.016	6.257	5.625	4.681	4.817	4.921
May	3.474	5.830	4.109	3.664	4.106	5.127	4.446	3.746	6.559	5.333	4.667	4.335	4.586
June	2.203	3.612	2.281	2.499	2.406	3.181	3.173	2.673	4.115	3.408	3.322	2.861	2.454
July	2.005	3.123	1.796	2.029	2.201	2.765	2.888	2.362	3.574	2.964	2.856	2.276	2.528
August	1.908	3.118	1.891	2.438	2.353	2.974	2.939	2.774	3.357	3.432	2.744	2.738	3.152
September	1.919	3.725	2.350	2.889	2.669	3.050	3.576	2.609	3.358	3.849	2.947	2.791	3.076
October	2.167	3.692	2.535	2.918	2.674	3.158	3.577	2.635	4.178	4.077	3.237	2.688	4.037
November	2.250	3.651	2.693	3.164	2.500	3.017	3.374	2.874	4.470	4.224	3.018	2.798	4.024
December	2.309	3.114	2.829	2.983	2.552	2.810	2.732	3.197	4.473	4.109	3.089	3.375	4.073

Table A2. Average monthly precipitation in 2016 at 13 meteorological stations (mm).

Month	Acheng	Bayan	Bin	Fangzheng	Urban	Hulan	Mulan	Shangzhi	Shuangcheng	Tonghe	Wuchang	Yanshou	Yilan
January	2.4	2.9	4.3	11	16.4	2.1	7.8	25.5	0.5	6.9	5.3	7.9	13.8
February	3.3	4.1	6.4	5.7	6.9	3.4	5.5	6.2	1.6	4.8	4.1	6.1	2.6
March	9	14.3	11.2	10.4	30.4	11.3	8.5	9.7	9	6	8.3	7	8.9
April	12.1	14.7	26.7	32.4	16.5	16.5	17.2	40.4	8.7	16.1	50.3	42.3	21.9
May	115.9	108.1	122.6	127	157.5	113.8	116	133.8	126.1	91	148.5	90.2	79
June	182.3	199.1	150.8	162.3	209.6	165.9	231.3	215.3	118.8	168.9	157.4	214.6	132.5
July	94.3	62.9	78.4	114.5	20.6	32.1	72.2	128.1	53.2	164.4	103.8	70.8	72.6
August	46.7	47.1	74.5	78.2	29.2	22.2	68.1	83.6	70	59.9	84.7	61.4	110.6
September	76.6	87.2	68	99.7	68.4	82.5	61.1	47.6	78.3	75.6	60	54.6	68.2
October	56.3	32.4	28.8	54.5	25.4	29.7	40.7	71.6	24.7	41	67.9	46.1	31.7
November	31.3	23.4	18.8	15.5	32	35.4	31.3	32.5	18.8	14.5	36.1	20.3	24.9
December	3	5.2	3.9	7.9	1.3	3	6.9	6.8	2.8	7.7	6.3	4	4.2

**Table A3.** Length of roads (km).

District	Highway	NR	PR	CR	TR	VR	Expressway	MR	SR	BR
Nangang	23.073	13.357	0	20.631	0	0	0	122.064	407.956	356.09
Daowai	37.497	17.796	0	25.797	0	0	0.7	114.38	355.788	332.346
Daoli	38.506	0	21.255	60.075	0	0	0.72	142.405	468.744	226.398
Xiangfang	46.573	19.845	0	41.538	0	0	0	137.000	377.521	349.519
Pingfang	0	19.576	0	22.56	0	0	0	7.495	229.556	101.487
Hulan	78.869	58.23	49.568	21.792	1033.261	0	15.416	34.731	0	711.068
Shuangcheng	59.391	61.746	0	238.827	1224.197	0	0	0.248	0	730.579
Songbei	49.711	64.983	0	17.582	666.639	0	42.995	11.017	0	312.628
Acheng	81.164	81.029	0	288.597	439.887	0	0	78.088	0	851.524
Wuchang	0	194.108	64.004	277.208	1186.617	2585.197	0	0	0	0
Shangzhi	118.885	183.914	58.633	348.773	592.282	1221.474	0	0	0	0
Bin	99.148	96.656	0	106.866	881.293	1581.849	0	0	0	0
Yanshou	0	0	57.237	90.023	361.279	682.83	0	0	0	0
Fangzheng	115.617	101.448	70.375	5.159	413.789	451.275	0	0	0	0
Yilan	135.204	83.269	123.768	5.315	623.746	845.294	0	0	0	0
Tonghe	0	0	195.2	0	373.72	452.602	0	0	0	0
Mulan	0	0	57.175	113.368	191.913	547.788	0	0	0	0
Bayan	18.284	0	33.745	230.94	1017.813	963.919	0	0	0	0
Total	901.922	995.957	730.96	1915.051	9009.436	9332.228	59.831	647.428	1839.565	3971.639

**Table A4.** The number of days without dust in Harbin 2016.

Month	Acheng	Bayan	Bin	Fangzheng	Urban	Hulan	Mulan	Shangzhi	Shuangcheng	Tonghe	Wuchang	Yanshou	Yilan
January	1	2	2	4	2	2	3	4	0	2	2	3	3
February	2	3	3	6	4	4	5	4	3	4	6	5	2
March	2	4	3	4	6	3	3	5	2	4	5	4	3
April	4	4	5	4	6	4	5	7	5	9	7	8	5
May	16	15	15	18	13	15	16	14	15	18	15	18	16
June	20	19	19	17	19	18	19	22	16	18	20	20	20
July	11	8	10	10	8	8	9	12	7	9	8	10	11
August	6	8	6	7	6	6	9	8	6	10	6	7	9
September	12	9	12	12	13	13	13	12	11	17	14	14	14
October	11	9	9	9	9	8	8	11	10	9	9	9	6
November	7	8	7	9	9	8	12	8	8	6	8	7	8
December	2	4	2	5	2	2	5	4	2	3	3	4	4
Total	94	93	93	105	97	91	107	111	85	109	103	109	101

## References

1. Tariq, S.; Loy-Benitez, J.; Nam, K.; Lee, G.; Kim, M.; Park, D.; Yoo, C. Transfer learning driven sequential forecasting and ventilation control of PM<sub>2.5</sub> associated health risk levels in underground public facilities. *J. Hazard. Mater.* **2021**, *406*, 124753. [[CrossRef](#)] [[PubMed](#)]
2. Lin, A.Q.; Zeng, Z.T.; Xu, Z.Y.; Li, X.D.; Chen, X.W.; Xu, W.J.; Liang, J.; Chen, G.J.; Li, X.; Shi, Z.; et al. Changes in the PM<sub>2.5</sub>-related environmental health burden caused by population migration and policy implications. *J. Clean. Prod.* **2021**, *287*, 125051.
3. Li, T.; Bi, X.; Dai, Q.; Liu, B.; Han, Y.; You, H.; Wang, L.; Zhang, J.; Cheng, Y.; Zhang, Y.; et al. Improving spatial resolution of soil fugitive dust emission inventory using RS-GIS technology: An application case in Tianjin, China. *Atmos. Environ.* **2018**, *191*, 46–54.
4. Li, Y.X.; Lv, C.; Yang, N.; Liu, H.; Liu, Z.L. A study of high temporal-spatial resolution greenhouse gas emissions inventory for on-road vehicles based on traffic speed-flow model: A case of Beijing. *J. Clean. Prod.* **2020**, *277*, 122419. [[CrossRef](#)]
5. Liu, Y.H.; Ma, J.L.; Li, L.; Lin, X.F.; Xu, W.J.; Ding, H. A high temporal-spatial vehicle emission inventory based on detailed hourly traffic data in a medium-sized city of China. *Environ. Pollut.* **2018**, *236*, 324–333. [[PubMed](#)]
6. Wiedinmyer, C.; Akagi, S.K.; Yokelson, R.J.; Emmons, L.K.; Al-Saadi, J.A.; Orlando, J.J.; Soja, A.J. The fire inventory from NCAR (FINN): A high resolution global model to estimate the emissions from open burning. *Geosci. Model Dev.* **2011**, *4*, 625–641. [[CrossRef](#)]
7. Xing, X.F.; Zhou, Y.; Lang, J.L.; Chen, D.S.; Cheng, S.Y.; Han, L.H.; Huang, D.W.; Zhang, Y.Y. Spatiotemporal variation of domestic biomass burning emissions in rural China based on a new estimation of fuel consumption. *Sci. Total Environ.* **2018**, *626*, 274–286. [[CrossRef](#)] [[PubMed](#)]
8. Liu, A.B.; Wu, Q.Z.; Cheng, X. Using the Google Earth Engine to estimate a 10 m resolution monthly inventory of soil fugitive dust emissions in Beijing, China. *Sci. Total Environ.* **2020**, *735*, 139174. [[CrossRef](#)]
9. Shen, Z.X.; Sun, J.; Cao, J.J.; Zhang, L.M.; Zhang, Q.; Lei, Y.L.; Gao, J.J.; Huang, R.J.; Liu, S.X.; Huang, Y.; et al. Chemical profiles of urban fugitive dust PM<sub>2.5</sub> samples in Northern Chinese cities. *Sci. Total Environ.* **2016**, *569*, 619–626. [[CrossRef](#)] [[PubMed](#)]
10. Tao, J.; Zhang, L.M.; Cao, J.J.; Zhang, R.J. A review of current knowledge concerning PM<sub>2.5</sub> chemical composition, aerosol optical properties and their relationships across China. *Atmos. Chem. Phys.* **2017**, *17*, 9485–9518. [[CrossRef](#)]
11. Cao, J.J.; Shen, Z.X.; Chow, J.C.; Watson, J.G.; Lee, S.C.; Tie, X.X.; Ho, K.F.; Wang, G.H.; Han, Y.M. Winter and summer PM<sub>2.5</sub> chemical compositions in fourteen Chinese cities. *J. Air Waste Manag. Assoc.* **2012**, *62*, 1214–1226. [[CrossRef](#)] [[PubMed](#)]
12. Kupiainen, K.; Denby, B.R.; Gustafsson, M.; Johansson, C.; Ketzel, M.; Kukkonen, J.; Norman, M.; Pirjola, L.; Sundvor, I.; Bennet, C.; et al. *Road Dust and PM<sub>10</sub> in the Nordic Countries. Measures to Reduce Road Dust Emissions from Traffic*; Nordic Council of Ministers: Copenhagen, Denmark, 2016.
13. Chen, S.Y.; Zhang, X.R.; Lin, J.T.; Huang, J.P.; Zhao, D.; Yuan, T.G.; Huang, K.N.; Luo, Y.; Jia, Z.; Zang, Z.; et al. Fugitive road dust PM<sub>2.5</sub> emissions and their potential health impacts. *Environ. Sci. Technol.* **2019**, *53*, 8455–8465. [[CrossRef](#)] [[PubMed](#)]
14. USEPA. *AP-42, Appendix C.1. Procedures for Sampling Surface/Bulk Dust Loading*, 5th ed.; U.S. Environmental Protection Agency: Washington, DC, USA, 2003.
15. USEPA. *AP-42, Appendix C.2. Procedures for Sampling Surface/Bulk Dust Loading*, 5th ed.; U.S. Environmental Protection Agency: Washington, DC, USA, 2003.
16. Jiang, N.; Dong, Z.; Xu, Y.Q.; Yu, F.; Yin, S.S.; Zhang, R.Q.; Tang, X.Y. Characterization of PM<sub>10</sub> and PM<sub>2.5</sub> Source Profiles of Fugitive Dust in Zhengzhou, China. *Aerosol. Air Qual. Res.* **2018**, *18*, 314–329. [[CrossRef](#)]
17. Cesari, D.; Contini, D.; Genga, A.; Siciliano, M.; Elefante, C.; Baglivi, F.; Daniele, L. Analysis of raw soils and their re-suspended PM<sub>10</sub> fractions: Characterisation of source profiles and enrichment factors. *Appl. Geochem.* **2012**, *27*, 1238–1246. [[CrossRef](#)]
18. Ning, D.T.; Zhong, L.X.; Chung, Y.S. Aerosol size distribution and elemental composition in urban areas of northern China. *Atmos. Environ.* **1996**, *30*, 2355–2362. [[CrossRef](#)]
19. Zhang, X.X.; Shi, P.J.; Liu, L.Y.; Tang, Y.; Cao, H.W.; Zhang, X.N.; Hu, X.; Guo, L.L.; Lue, Y.L.; Qu, Z.Q.; et al. Ambient TSP concentration and dustfall in major cities of China: Spatial distribution and temporal variability. *Atmos. Environ.* **2010**, *44*, 1641–1648. [[CrossRef](#)]
20. Sun, J.; Shen, Z.; Zhang, L.; Lei, Y.; Gong, X.; Zhang, Q.; Zhang, T.; Xu, H.; Cui, S.; Wang, Q.; et al. Chemical source profiles of urban fugitive dust PM<sub>2.5</sub> samples from 21 cities across China. *Sci. Total Environ.* **2019**, *649*, 1045–1053. [[CrossRef](#)]
21. Zhou, Y.; Xing, X.F.; Lang, J.L.; Chen, D.S.; Cheng, S.Y.; Wei, L.; Wei, X.; Liu, C. A comprehensive biomass burning emission inventory with high spatial and temporal resolution in China. *Atmos. Chem. Phys.* **2017**, *17*, 2839–2864. [[CrossRef](#)]
22. Kuhns, H.; Etyemezian, V.; Landwehr, D.; MacDougall, C.; Pitchford, M.; Green, M. Testing Re-entrained Aerosol Kinetic Emissions from Roads (TRAKER): A new approach to infer silt loading on roadways. *Atmos. Environ.* **2001**, *35*, 2815–2825. [[CrossRef](#)]
23. Gao, C.; Gao, W.; Song, K.; Na, H.; Tian, F.; Zhang, S. Spatial and temporal dynamics of air-pollutant emission inventory of steel industry in China: A bottom-up approach. *Resour. Conserv. Recycl.* **2019**, *143*, 184–200. [[CrossRef](#)]
24. Philip, S.; Martin, R.V.; Snider, G.; Weagle, C.L.; van Donkelaar, A.; Brauer, M.; Henze, D.K.; Klimont, Z.; Venkataraman, C.; Guttikunda, S.K.; et al. Anthropogenic fugitive, combustion and industrial dust is a significant, underrepresented fine particulate matter source in global atmospheric models. *Environ. Res. Lett.* **2017**, *12*, 044018. [[CrossRef](#)]

25. Zhao, H.T.; Li, X.Y.; Wang, X.M. Heavy Metal Contents of Road-Deposited Sediment along the Urban-Rural Gradient around Beijing and its Potential Contribution to Runoff Pollution. *Environ. Sci. Technol.* **2011**, *45*, 7120–7127. [[CrossRef](#)] [[PubMed](#)]
26. Fan, S.; Tian, G.; Cheng, S.; Qin, J. A new approach to developing a fugitive road dust emission inventory and emission trend from 2006 to 2010 in the Beijing metropolitan area, China. *J. Environ. Qual.* **2013**, *42*, 1039–1045. [[CrossRef](#)] [[PubMed](#)]
27. Yin, S.; Zheng, J.; Lu, Q.; Yuan, Z.; Huang, Z.; Zhong, L.; Lin, H. A refined 2010-based VOC emission inventory and its improvement on modeling regional ozone in the Pearl River Delta Region, China. *Sci. Total Environ.* **2015**, *514*, 426–438. [[CrossRef](#)] [[PubMed](#)]
28. Kim, N.K.; Kim, Y.P.; Morino, Y.; Kurokawa, J.; Ohara, T. Verification of NO<sub>x</sub> emission inventories over North Korea. *Environ. Pollut.* **2014**, *195*, 236–244. [[CrossRef](#)]
29. Lindhjem, C.E.; Pollack, A.K.; DenBleyker, A.; Shaw, S.L. Effects of improved spatial and temporal modeling of on-road vehicle emissions. *J. Air Waste Manag. Assoc.* **2012**, *62*, 471–484. [[CrossRef](#)] [[PubMed](#)]
30. Norman, M.; Sundvor, I.; Denby, B.R.; Johansson, C.; Gustafsson, M.; Blomqvist, G.; Janhall, S. Modelling road dust emission abatement measures using the NORTRIP model: Vehicle speed and studded tyre reduction. *Atmos. Environ.* **2016**, *134*, 96–108. [[CrossRef](#)]
31. Peng, K.; Yang, Y.; Zheng, J.; Yin, S.; Gao, Z.; Huang, X. Emission factor and inventory of paved road fugitive dust sources in the Pearl River Delta region. *Acta Sci. Circumstantiae* **2013**, *33*, 2657–2663.
32. Yang, D.; Ye, Z.; Yang, H.; Song, Y. Emission inventory and spatial distribution of paved road fugitive dust in Chengdu in Sichuan Province. *Environ. Eng.* **2015**, *33*, 83–87.
33. Jiang, P.Y.; Zhong, X.; Li, L.Y. On-road vehicle emission inventory and its spatio-temporal variations in North China Plain. *Environ. Pollut.* **2020**, *267*, 115639. [[CrossRef](#)]
34. Qi, J.; Zheng, B.; Li, M.; Yu, F.; Chen, C.; Liu, F.; Zhou, X.; Yuan, J.; Zhang, Q.; He, K. A high-resolution air pollutants emission inventory in 2013 for the Beijing-Tianjin-Hebei region, China. *Atmos. Environ.* **2017**, *170*, 156–168. [[CrossRef](#)]
35. Fan, S.; Qin, J.; Cai, Y. Road fugitive dust emission inventory in Huhhot urban area. *Environ. Sci. Manag.* **2011**, *36*, 19–22.
36. Xu, Y.; Zhou, Q. Emission characteristics and spatial distribution of road fugitive dust in Tianjin, China. *China Environ. Sci.* **2012**, *32*, 2168–2173.
37. Wang, S.; Wang, T.; Shi, R.; Tian, J. Estimation of different fugitive dust emission inventory in Nanjing. *J. Univ. Chin. Acad. Sci.* **2014**, *31*, 351–359.
38. Fan, S.; Zhang, D.; Tian, L.; Li, X.; Guo, J.; Lin, Y. Emission inventory and spatial distribution of road fugitive dust PM<sub>2.5</sub> in Beijing. *Res. Environ. Sci.* **2016**, *29*, 20–28.
39. Huo, H.; Zhang, Q.; He, K.B.; Wang, Q.D.; Yao, Z.L.; Streets, D.G. High-resolution vehicular emission inventory using a link-based method: A case study of light-duty vehicles in Beijing. *Environ. Sci. Technol.* **2009**, *43*, 2394–2399. [[CrossRef](#)]
40. Jing, B.; Wu, L.; Mao, H.; Gong, S.; He, J.; Zou, C.; Song, G.; Li, X.; Wu, Z. Development of a vehicle emission inventory with high temporal-spatial resolution based on NRT traffic data and its impact on air pollution in Beijing—Part 1: Development and evaluation of vehicle emission inventory. *Atmos. Chem. Phys.* **2016**, *16*, 3161–3170. [[CrossRef](#)]
41. Hao, J.M.; He, D.Q.; Wu, Y.; Fu, L.; He, K.B. A study of the emission and concentration distribution of vehicular pollutants in the urban area of Beijing. *Atmos. Environ.* **2000**, *34*, 453–465. [[CrossRef](#)]
42. Zheng, J.Y.; Che, W.W.; Wang, X.M.; Louie, P.; Zhong, L.J. Road-network-based spatial allocation of on-road mobile source emissions in the Pearl River Delta region, China, and comparisons with population-based approach. *J. Air Waste Manag. Assoc.* **2009**, *59*, 1405–1416. [[CrossRef](#)] [[PubMed](#)]